Journal of the Endocrine Society, 2023, **7**, 1–15
https://doi.org/10.1210/jendso/bvac186
Advance access publication 3 December 2022
Research Article

Progesterone Receptor–Mediated Regulation of Cellular Glucose and ^{18}F-Fluorodeoxyglucose Uptake in Breast Cancer

Kelley Salem,[1] Rebecca M. Reese,[2] Elaine T. Alarid,[2,3] and Amy M. Fowler[1,3,4]

[1]Department of Radiology, University of Wisconsin School of Medicine and Public Health, Madison, WI 53792, USA
[2]McArdle Laboratory for Cancer Research, Department of Oncology and Carbone Comprehensive Cancer Center, University of Wisconsin-Madison, Madison, WI 53705, USA
[3]University of Wisconsin Carbone Cancer Center, Madison, WI 53792, USA
[4]Department of Medical Physics, University of Wisconsin School of Medicine and Public Health, Madison, WI 53705, USA

Correspondence: Amy M. Fowler, MD, PhD, University of Wisconsin School of Medicine and Public Health, 600 Highland Avenue, Madison, WI 53792-3252, USA. Email: afowler@uwhealth.org.

Abstract

Context: Positron emission tomography imaging with 2-deoxy-2-[^{18}F]-fluoro-D-glucose (FDG) is used clinically for initial staging, restaging, and assessing therapy response in breast cancer. Tumor FDG uptake in steroid hormone receptor–positive breast cancer and physiologic FDG uptake in normal breast tissue can be affected by hormonal factors such as menstrual cycle phase, menopausal status, and hormone replacement therapy.

Objective: The purpose of this study was to determine the role of the progesterone receptor (PR) in regulating glucose and FDG uptake in breast cancer cells.

Methods and Results: PR-positive T47D breast cancer cells treated with PR agonists had increased FDG uptake compared with ethanol control. There was no significant change in FDG uptake in response to PR agonists in PR-negative MDA-MB-231 cells, MDA-MB-468 cells, or T47D PR knockout cells. Treatment of T47D cells with PR antagonists inhibited the effect of R5020 on FDG uptake. Using T47D cell lines that only express either the PR-A or the PR-B isoform, PR agonists increased FDG uptake in both cell types. Experiments using actinomycin D and cycloheximide demonstrated the requirement for both transcription and translation in PR regulation of FDG uptake. *GLUT1* and *PFKFB3* mRNA expression and the enzymatic activity of glucose-6-phosphate dehydrogenase and 6-phosphogluconate dehydrogenase were increased after progestin treatment of T47D cells.

Conclusion: Thus, progesterone and progestins increase FDG uptake in T47D breast cancer cells through the classical action of PR as a ligand-activated transcription factor. Ligand-activated PR ultimately increases expression and activity of proteins involved in glucose uptake, glycolysis, and the pentose phosphate pathway.

Key Words: progesterone receptor, ^{18}F-fluorodeoxyglucose (FDG), glycolysis, breast cancer, progestin, pentose phosphate pathway

Abbreviations: 2DG6P, 2-deoxyglucose-6-phosphate; 6PGD, 6-phosphogluconate dehydrogenase; ChIP, chromatin immunoprecipitation; CPM, counts per minute; DMEM, Dulbecco's modified Eagle's medium; ER, estrogen receptor; FDG, 2-deoxy-2-[^{18}F]-fluoro-D-glucose; GLUT, glucose transporter; GR, glucocorticoid receptor; LDH, lactate dehydrogenase; MA, megestrol acetate; MPA, medroxyprogesterone acetate; PBS, phosphate-buffered saline; PET, positron emission tomography; G6PD, glucose-6-phosphate dehydrogenase; MRI, magnetic resonance imaging; NADPH, nicotinamide adenine dinucleotide phosphate; PR, progesterone receptor; PRE, progesterone response element; PR KO, knockout of the *PGR* gene; RPMI, Roswell Park Memorial Institute; Scr, scrambled; SDS, sodium dodecyl sulfate; qPCR, quantitative real-time polymerase chain reaction; UPA, ulipristal acetate.

Approximately 70% of breast cancers are estrogen receptor (ER) and/or progesterone receptor (PR) positive [1, 2]. In breast cancer, PR is expressed as 2 predominant isoforms, PR-A and PR-B, using separate promoters of the *PGR* gene [3]. PR-B is the longer isoform, having an additional 164 amino acids in the N-terminus compared with PR-A [3]. The receptor isoforms have similar ligand binding and DNA binding functions; however, they differ in their transcriptional activity [4–6]. Generally, PR-B is a stronger regulator of transcription in response to progesterone than PR-A [4–6]. While there are genes regulated by both isoforms, many progesterone-regulated target genes are independently controlled by one isoform or the other [7]. Separate from the classic nuclear action of PR, rapid membrane-initiated signaling events can also be stimulated by progestins [8, 9]. Crosstalk between hormonal and metabolic signaling pathways have been hypothesized to be a major driving force for endocrine therapy resistance and metastasis [10].

Cancer cells have increased glucose metabolism and switch to using aerobic glycolysis for energy generation rather than the more efficient process of oxidative phosphorylation. This metabolic reprogramming, termed the "Warburg effect" [11–13], is a cancer hallmark that can be leveraged clinically using the glucose analog, 2-deoxy-2-[^{18}F]-fluoro-D-glucose

Received: 5 July 2022. **Editorial Decision:** 1 December 2022. **Corrected and Typeset:** 28 December 2022

(FDG) [14–16]. Like glucose, FDG is transported into the cell through facilitative glucose transporter (GLUT) proteins [17–20] and then phosphorylated by hexokinase to FDG-6-phosphate [21, 22]. Once phosphorylated, unlike glucose-6-phosphate, FDG-6-phosphate cannot be metabolized further through glycolysis due to the presence of ^{18}F instead of the 2-hydroxyl group [21, 22]. Due to low levels of glucose-6-phosphatase needed for dephosphorylation, FDG-6-phosphate cannot be released and is thus trapped intracellularly [21–23]. Accumulation of FDG can be visualized and quantified using positron emission tomography (PET) imaging. Clinically, FDG PET/computed tomography imaging can be used for initial staging, restaging, and assessing therapy response for patients with breast cancer [24].

Physiologic FDG uptake in normal breast tissue is affected by hormonal factors. Studies using whole-body PET imaging, as well as high-resolution dedicated breast PET devices, have demonstrated higher physiologic FDG uptake in normal breast tissue of premenopausal women compared with postmenopausal women [25–28]. Furthermore, physiologic FDG uptake in normal breast tissue of postmenopausal women taking hormone replacement therapy was similar to premenopausal women [25]. The specific composition of the hormone replacement therapy used in that study was not reported. Furthermore, a weak but significant positive correlation between serum progesterone level and FDG uptake was demonstrated in the contralateral normal breast tissue of premenopausal women with breast cancer. No significant correlation was found between serum estradiol levels and FDG uptake [29]. A significant correlation between menstrual cycle phase and FDG uptake was seen in normal breast, with higher uptake during the secretory/luteal phase when progesterone levels peak from the corpus luteum [28, 30–32]. Collectively, these clinical studies provide indirect evidence for a role of steroid hormones, particularly progesterone, in FDG uptake of normal breast tissue.

FDG uptake in steroid hormone receptor positive breast cancer can also be influenced by fluctuating hormonal levels. A correlation between FDG uptake and menstrual cycle for luminal A subtype tumors (ER+/HER2−, Ki67 < 14%, PR ≥ 20%) was demonstrated, with maximum standardized uptake values significantly higher for patients during the periovulatory/luteal phase than for those during the follicular phase [33]. However, tumor FDG uptake was not significantly different between the menstrual phases for patients with luminal B (ER+/HER2−, Ki67 > 14%, PR < 20%) or nonluminal tumors [33].

The role of progesterone and its signaling through PR in regulating FDG uptake has not been defined. The aim of this study was to determine the role PR has in regulating glucose and FDG uptake in breast cancer cells via pharmacologic and genomic-based approaches. Given growing evidence of PR and ER crosstalk in breast cancer tumor biology [34–36] and current clinical trials testing new antiprogestin therapeutics selectively targeting PR [37–40], a better understanding of how ligand-activated PR influences FDG uptake could be helpful for using PET/computed tomography imaging to predict and monitor therapy response.

Materials and Methods

Cell Culture

Experiments were performed under a protocol approved by the University of Wisconsin-Madison Office of Biological Safety. T47D, MDA-MB-231, and MDA-MB-468 cells were obtained from American Type Culture Collection. Modified T47D cell lines were also used including those with CRISPR knockout of the *PGR* gene (PR KO) and the scrambled (Scr) control [41], and cell lines expressing only the PR-A protein isoform (T47D YA) or the PR-B protein isoform (T47D YB) [42]. Cell lines were authenticated using short tandem repeat analysis and tested negative for murine pathogens and *Mycoplasma* contamination. All T47D cells were cultured in Roswell Park Memorial Institute media (RPMI 1640 with L-glutamine; Corning 10-040-CV). MCF-7, MDA-MB-231, and MDA-MB-468 cells were cultured in Dulbecco's Modified Eagle medium (DMEM with 4.5 g/L glucose, L-glutamine, sodium pyruvate; Corning 10-013-CV). Media was supplemented with 10% fetal bovine serum (VWR) and 1% penicillin–streptomycin (GeminiBio). Cells were maintained at either 5% or 10% CO_2 at 37 °C. For hormone deprivation, cells were grown in phenol red–free media (Corning DMEM 17-205-CV or RPMI 17-205-CV) supplemented with 5% charcoal–dextran stripped fetal bovine serum, 2% L-glutamine, and 1% penicillin–streptomycin. Cells were trypsinized using phenol red–free trypsin (0.05%, Gibco).

FDG Cell Uptake Assay

Cells were hormone starved for 3 days, then seeded into a 24-well plate at a density of 4×10^4 cells in a total of 0.5 mL of medium. Parallel wells were seeded for protein measurement. The following day, cells were treated with various hormones: 0.01 to 100 nM promegestone (R5020, Perkin Elmer), 100 nM medroxyprogesterone acetate (MPA, Steraloids), 100 nM megestrol acetate (MA, Steraloids), 100 nM mifepristone (RU486, Sigma), 100 nM ulipristal acetate (UPA, Sigma), 100 nM progesterone (Sigma), or 100 nM dexamethasone (Sigma). For experiments testing the requirement of transcription and translation, cells were pretreated with actinomycin D (1 μM; Sigma) or cycloheximide (10 μg/mL; Sigma) for 1 hour prior to the addition of hormone. Thirty minutes prior to the assay, cells were washed twice with phosphate-buffered saline (PBS) and placed into either no glucose or high glucose (4.5 g/L) DMEM medium without glutamine or phenol red (Gibco A14430-01 or 31053-028, respectively) containing the same treatment. FDG (1 μCi, Sofie) was added to cells and incubated for 40 minutes at 37 °C. After the incubation, the medium was removed, cells were washed with PBS, and then lysed with 1 N NaOH. Radioactivity was measured using a gamma counter (PerkinElmer) and decay corrected and normalized to protein content. Specific FDG uptake was determined by subtracting the values of the high glucose medium lysates (nonspecific activity) from the corresponding no glucose medium lysates (total activity). Protein concentration was determined using the Bradford assay.

Glucose Consumption and Glucose Uptake Assays

Cells were hormone deprived for 3 days and then seeded at a density of 1×10^5 cells per well. Cells were treated with 100 nM R5020, MPA, MA, or ethanol vehicle (0.1%, v/v) for 24 hours. Cellular glucose consumption was measured using a point-of-care glucometer (AccuChek) and determined by subtracting the glucose value measured in wells with medium alone, without cells, from the glucose value measured in

medium from wells containing cells with the respective treatments. Cells were counted and the amount of glucose consumed was determined on a per-cell basis. Glucose uptake was also determined by measuring 2-deoxyglucose-6-phosphate (2DG6P) using the nonradioactive Glucose Uptake-Glo bioluminescent assay (Promega). Cells were hormone deprived for 3 days and seeded at a density of 4×10^4 per well in a 96-well white plate with a clear bottom. Cells were treated with or without 100 nM R5020 for 24 hours and the assay was performed following the manufacturer's protocol. Data were normalized to protein content and expressed as fold change relative to ethanol control.

Reporter Gene Assays

Cells were hormone deprived for 3 days, seeded, and cotransfected with a progesterone response element (PRE) firefly luciferase reporter gene plasmid [43] and a beta-galactosidase control plasmid [44] using Lipofectamine 3000 for 5 hours (Invitrogen). The next day, cells were treated with hormones. After treatment, cells were washed and harvested. Luciferase activity (Promega) and beta-galactosidase activity (Applied Biosystems) assays were performed using the manufacturers' protocols.

Flow Cytometry

T47D cells were hormone deprived for 3 days. Cells were treated for 24 hours with either 100 nM progesterone, R5020, or ethanol. Cells were harvested, washed with PBS, and fixed in 70% ethanol. Fixed cells were stained with 50 µg/mL propidium iodine (Sigma-Aldrich) containing 100 µg/mL RNase (Sigma-Aldrich) overnight at 4 °C. Cell cycle analysis was performed using Attune NxT (ThermoFisher) flow cytometer and data were analyzed using FlowJo software (FlowJo, LLC).

Western Blot Analysis

Cells were lysed in radioimmunoprecipitation assay buffer containing protease inhibitors (Sigma) and phosphatase inhibitors (Sigma). Protein concentration was measured using Bradford Reagent (Bio-Rad) and equal amounts of protein were run on 10% sodium dodecyl sulfate (SDS)-polyacrylamide gel electrophoresis gels. Protein was transferred to PVDF and incubated with antibodies against PR (1:1000; Leica Biosystems Cat# NCL-L-PGR-312, RRID:AB_563967) or β-actin (1:10 000; Sigma-Aldrich Cat# A1978, RRID:AB_476692). Protein expression was quantified using ImageJ (1.48 V).

Quantitative Real-Time Polymerase Chain Reaction

Cells were grown in hormone depleted media for 72 hours and plated in 6 well plates at a density of 3.75×10^5 cells per well. Cells were treated with 10 nM R5020 for varying incubation times. RNA was extracted using RNeasy (Qiagen) and cDNA was synthesized using iScript DNA synthesis (Bio-Rad). Primer sequences are as follows—*FKBP54*: forward 5′-AGAACCAAACGGAAAGGAGAG-3′ and reverse 5′-TCACCGCCTGCATGTATTT-3′; *HK2*: forward 5′-GGGACAATGGATGCCTAGATG-3′ and reverse 5′-GTTACGGACAATCTCACCCAG-3′; *G6PD*: forward 5′-CCCGGAAACGGTCGTACACT-3′ and reverse 5′-CATGACGCTGTCTGCGCTTC-3′; *PFKFB3*: forward 5′-GGCAAGACCTACATCTCCAAG-3′ and reverse 5′-ATGGCTTCCTCATTGTCGG-3′; *SLC2A1 (GLUT1)*: forward 5′-TCATCGTGGCTGAACTCTTC-3′ and reverse 5′-GATGAAGACGTAGGGACCAC-3′; *SLC2A4 (GLUT4)*: forward 5′-TCGGTTCTTTCATCTTCGCC-3′ and reverse 5′-AGAACACAGCAAGGACCAG-3′; *SLC2A12 (GLUT12)*: forward 5′-TTGCTTGTTTATGTTGCTGCT-3′ and reverse 5′-AGATTGATGCCCCAGTTCATG-3′; and *RPLP0*: forward 5′-CCATTCTATCATCAACGGGTACAA-3′ and reverse 5′-TCAGCAAGTGGGAAGGTGTAATC-3′. C_T values were normalized to the housekeeping gene, *RPLP0*. Relative fold change was calculated using the formula $2^{-\Delta\Delta C_T}$ [45].

Glucose-6-Phosphate Dehydrogenase and 6-Phosphogluconate Dehydrogenase Activity Assays

T47D cells were hormone deprived for 3 days prior to experimentation. Cells were seeded and treated with 100 nM R5020 for 24 hours. The cells were washed twice with ice cold PBS, scraped into 1 mL of PBS, and pelleted. Glucose-6-phosphate dehydrogenase (G6PD) and 6-phosphogluconate dehydrogenase (6PGD) activity assays were performed at the University of Iowa Free Radical and Radiation Biology core. Cell pellets were lysed in diethylenetriaminepentaacetic acid (DETAPAC) buffer. For each sample, 2 cuvettes were prepared—one for total activity (G6PD + 6PGD) and another for 6PGD activity. For total activity, substrate was added that consisted of 750 µL of nicotinamide adenine dinucleotide phosphate (NADP) reagent (2 mM $NADP^+$ in 100 mM Tris buffer, pH 8.0 with 1 mM $MgCl_2$), 100 µL of G6P (12 mM D-glucose 6 phosphate in ddH_2O), and 100 µL of 6PGA (12 mM 6-phosphogluconic acid in ddH_2O). For the 6PGD activity, 750 µL of NADP reagent, 100 µL of ddH_2O, and 100 µL of 6PGA were added. Cuvettes were incubated for 5 minutes at 37 °C prior to samples being added. Within each cuvette, 50 µL of sample was added and mixed. NADPH formation was measured at 340 nm for 5 minutes. G6PD activity was calculated by subtracting the 6PGD activity from the total activity.

PR Binding Site Identification and Motif Analysis

Raw sequencing data of PR DNA-binding sites following treatment with R5020 in T47D cells was acquired from a previous publication (GEO accession number GSE68359) [35]. Reads were aligned to the hg38 genome using Bowtie2 [46]. Peaks were called with MACS2 [47] using input data as a control and false discovery rate of 0.05. PR binding sites were annotated to the nearest gene using Genomic Regions Enrichment of Annotations Tool (GREAT, version 4.0.4 [48]) with a gene association rule of "two nearest genes" and default settings. Binding sites were then filtered for those within 100 kb of the nearest transcription start site. Motif analysis was performed using the Find Individual Motif Occurrences (FIMO) software tool [49] in the Multiple Expectation maximizations for Motif Elicitation (MEME) Suite [50].

Chromatin Immunoprecipitation

T47D cells were hormone deprived for 3 days then were treated with either 10 nM R5020 or ethanol vehicle for 3 hours. Samples were prepared for chromatin

immunoprecipitation (ChIP) as previously described [51]. Precleared chromatin was subjected to immunoprecipitation with PR A/B rabbit monoclonal antibody (1:100; Cell Signaling Cat# 8757, RRID:AB_2797144) or rabbit IgG control and incubated overnight at 4 °C while rotating. A bolus (45 µL) of 50% Protein Sepharose A beads (Cytiva) was then added and incubated for 1 hour at 4 °C. The precipitated complexes were washed once with 1 mL of TSE I buffer (0.1% SDS, 1% Triton X-100, 2 mM EDTA, 20 mM Tris-HCl pH 8.1, 150 mM NaCl), once with 1 mL of TSE II buffer (0.1% SDS, 1% Triton X-100, 2 mM EDTA, 20 mM Tris-HCl pH 8.1, 500 mM NaCl), once with 1 mL of TSE III Buffer (0.25 M LiCl, 1% NP-40, 1% sodium deoxycholate, 10 mM Tris-HCl pH 8.1), and twice with 1 mL of TE (10 mM Tris-HCl pH 8.1, 1 mM EDTA). Chromatin complexes were extracted from beads by incubating in 75 µL of extraction buffer (1% SDS, 0.1 M $NaHCO_3$) for 30 minutes. Extraction was repeated 3 times and the extractions were pooled. Samples were reverse cross-linked by adding 10 µL of 5 M NaCl to each sample and incubating at 65 °C overnight. The next day, 4.2 µL of Proteinase K (Qiagen) was added and samples were incubated at 65 °C for 1 hour. DNA was purified using the QIAquick PCR Purification Kit (Qiagen) and 1 µL of the purified DNA was analyzed via quantitative real-time polymerase chain reaction (qPCR). Data are calculated as a percent of input. Primers used for ChIP-qPCR were *PFKFB3*: forward 5′-CCCAGCATCCC CTTACACAG-3′ and reverse 5′-CGTCCCAGGTTGAAGG ACAT-3′; *SLC2A1 (GLUT1)*: forward 5′-TGGTGCCTTCC TTCCCATTG-3′ and reverse 5′-CTGCTGACTTGGGAC AGGTT-3′; and *SYNE1*: forward 5′-AACGGGAATCC AACTAAGCCT-3′ and reverse 5′-CCATAACCTGTC GCAGAAGC-3′.

Statistical Analysis

Data represent the mean ± SEM of 3 independent experiments. Statistical analysis was performed using GraphPad Prism 7.0 software. Unpaired t tests and 1-way analysis of variance with multiple comparison post-tests were used to compare treatment effect relative to the ethanol controls. An unpaired t-test was used to compare PR protein levels in T47D YA and T47D YB cells.

Results

PR Agonists Stimulate FDG Uptake and Glucose Uptake in T47D Breast Cancer Cells

To determine the effect of ligand-activated PR on FDG uptake, three PR agonists were used—promegestone (R5020), MPA, and MA. T47D, MDA-MB-231, and MDA-MB-468 cells were hormone deprived for 3 days and then were treated with either R5020, MPA, MA (each 100 nM), or ethanol (0.1% v/v) for 24 hours. Cells were then incubated with 1 µCi of FDG for 40 minutes and retained radioactivity was measured. In the PR-positive T47D cells, FDG uptake was significantly increased by R5020 ($12.9 \pm 1.2 \times 10^5$ CPM/mg protein, $P = .01$), MPA ($16.6 \pm 1.2 \times 10^5$ CPM/mg protein, $P = .003$), and MA ($16.3 \pm 1.2 \times 10^5$ CPM/mg protein, $P = .003$) vs ethanol control ($6.9 \pm 0.8 \times 10^5$ CPM/mg protein; Fig. 1A). However, no progestin hormonal effect was observed in the PR-positive MCF-7 cell line (Fig. 1B) or PR-negative cell lines MDA-MB-231 (Fig. 1C) or MDA-MB-468 (Fig. 1D). PR transactivation by R5020 was confirmed using a reporter gene assay (Fig. 1E) which showed stronger PR transcriptional activity in T47D cells than in MCF-7 cells and no progestin effect in MDA-MB-231 and MDA-MB-468 cells. Treatment with the natural PR agonist, progesterone (100 nM for 24 hours), increased FDG uptake in T47D cells similar to the response observed with synthetic progestins (1.8 ± 0.2 fold increase compared with ethanol control, $P = .02$). However, treatment of T47D cells with 100 nM dexamethasone, a glucocorticoid receptor (GR) agonist, for 24 hours had no effect on FDG uptake compared with ethanol (1.0 ± 0.2 fold change vs 1.0 ± 0.2, $P = 1.0$, Fig. 1F). Treatment with R5020 or progesterone for 24 hours significantly decreased the percentage of T47D cells in G0/G1 and increased the percentage of cells in G2 compared with ethanol control (Table 1). Taken together, FDG uptake is increased after PR agonist treatment in T47D cells.

Glucose Uptake in T47D Cells Is Increased After PR Agonist Treatment

To confirm FDG uptake, glucose consumption was also measured in T47D cells after 24 hours treatment with PR agonists using a glucometer. There was a significant increase in glucose consumed after R5020 and MPA treatment compared with ethanol (1.9 ± 0.3 fold change, $P = .04$ and 1.9 ± 0.2 fold change, $P = .02$ vs 1.0 ± 0.2, respectively, Fig. 2A). MA treatment resulted in a nonsignificant increase in glucose consumption (1.7 ± 0.3 fold increase). Additionally, glucose uptake based on 2DG6P formation was significantly increased in T47D cells treated with R5020 (100 nM) compared with ethanol (1.7 ± 0.2 fold change vs 1.0 ± 0.07, $P = .03$; Fig. 2B). Taken together, these data show that PR agonists increase glucose consumption and glucose uptake in T47D cells in confirmation with FDG uptake.

Dynamics of R5020 Induction of FDG Uptake

To define the dynamics of ligand activated PR on FDG uptake, dose titration and time course experiments were performed. Hormone-deprived T47D cells were treated with R5020 (10^{-11} to 10^{-7} M) for 24 hours. FDG uptake was measured and PR transactivation confirmed with a reporter gene assay (Fig. 3A and 3B). Sigmoidal dose–response curves were observed for both FDG uptake (Fig. 3A) and PR transcriptional activity (Fig. 3B) with half maximal effective concentration values of 0.2 nM (95% CI 0.03-1.6 nM) and 0.07 nM (95% CI 0.04-1.2 nM), respectively. FDG uptake and PR transcriptional activity were then measured in T47D cells treated with a saturating dose of 100 nM R5020 for 0.5, 4, 8, 12, 24, 36, and 48 hours (Fig. 3C and 3D). A significant increase in FDG uptake was observed at 12 hours with a 1.9-fold increase compared with ethanol control and was sustained through 48 hours of treatment. Similar to the results obtained with R5020, treatment of T47D cells with 100 nM progesterone for 0.5 hours did not cause an increase in FDG uptake compared with ethanol (0.8 ± 0.1 fold change vs 1.0 ± 0.09; $P = .9$).

Progestins Increase FDG Uptake Through PR-A or PR-B

While PR exists in several isoforms, the two predominant isoforms with distinct roles in breast cancer biology are PR-A and

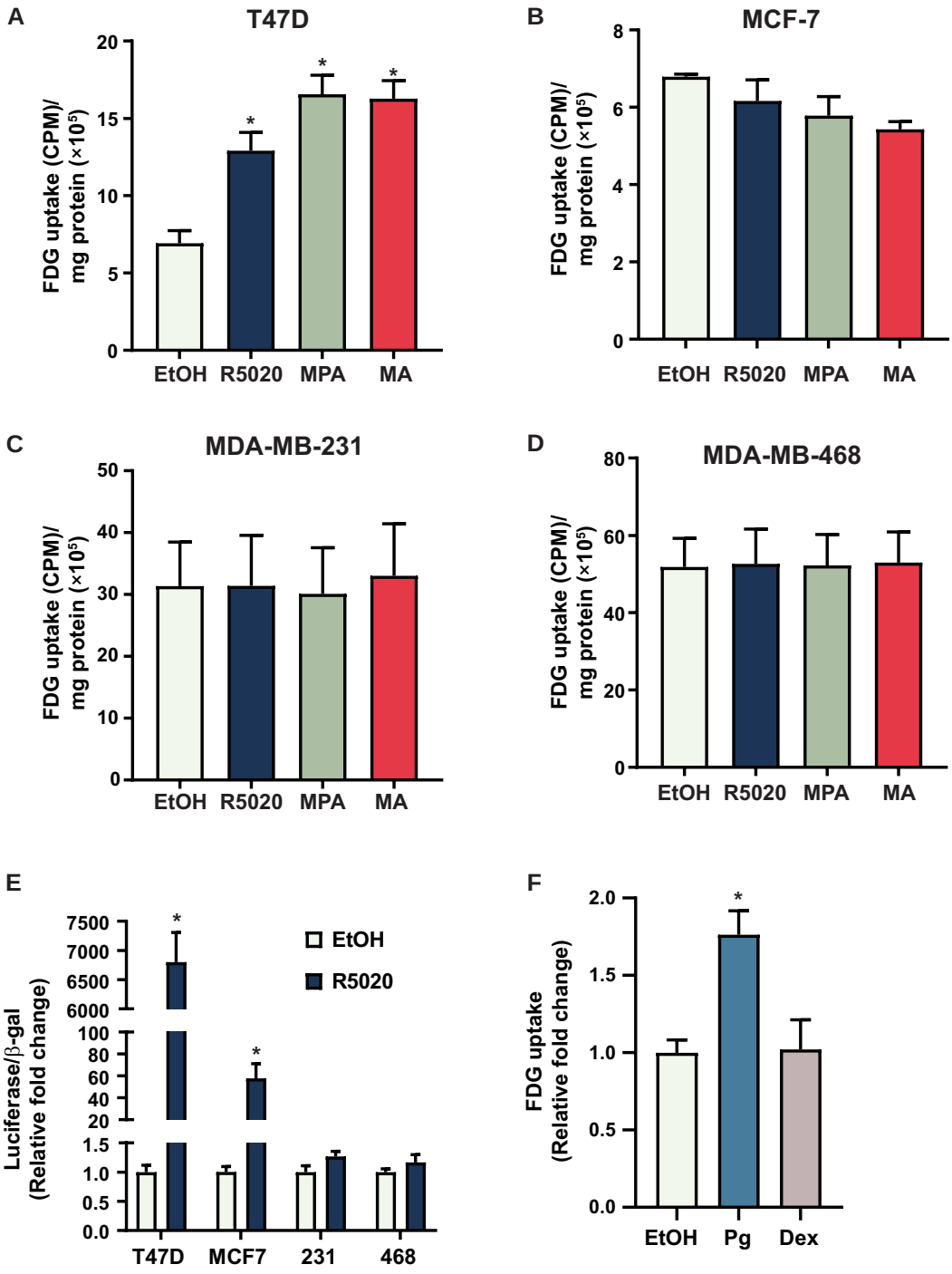

Figure 1. PR agonist induction of FDG uptake in T47D cells. Cells were steroid hormone deprived for 3 days prior to experimentation then seeded, and the next day treated with 100 nM R5020, medroxyprogesterone acetate (MPA), megestrol acetate (MA), or ethanol (EtOH) control. After treatment, FDG uptake assay was performed in (A) T47D, (B) MCF-7, (C) MDA-MB-231, and (D) MDA-MB-468 cells. Thirty minutes prior to the addition of 1 μCi FDG, cells were washed with PBS and placed in medium with or without glucose plus the treatment. Cells were incubated with FDG for 40 minutes, then washed and lysed, and radioactivity was measured. Specific FDG uptake was calculated and normalized to protein content. (E) Reporter gene assay for PR transcriptional activation after 24 hours treatment with 100 nM of R5020 or ethanol control. (F) FDG uptake was measured in T47D cells after 24 hours treatment with 100 nM progesterone (Pg) or dexamethasone (Dex). Data represents the mean ± SEM of 3 independent experiments. * $P < .05$ compared with ethanol.

PR-B. To determine if one isoform is responsible for the increase in FDG uptake due to PR agonists, T47D cells that stably express either PR-A (T47D YA) or PR-B (T47D YB) were used. Cells were hormone deprived for 3 days and then treated with PR agonists at 100 nM for 24 hours (Fig. 4A). T47D YA cells treated with R5020, MPA, and MA had an increase in FDG uptake compared with ethanol vehicle ($7.4 \pm 0.5 \times 10^5$ CPM/mg protein, $P = .02$; $8.0 \pm 0.6 \times 10^5$ CPM/mg protein, $P = .01$; $7.1 \pm 1.2 \times 10^5$ CPM/mg protein, $P = .03$ vs $3.4 \pm 0.8 \times 10^5$ CPM/mg protein, respectively). Similarly, R5020 ($13.0 \pm 0.6 \times 10^5$ CPM/mg protein, $P = .0001$), MPA ($12.5 \pm 1.2 \times 10^5$ CPM/mg protein, $P = .0002$), and MA (13.1 ± 0.5

Table 1. Cell cycle analysis in T47D cells

	G0/G1	S	G2
EtOH	58.0 ± 1.0	18.9 ± 1.1	13.7 ± 0.5
R5020	43.5 ± 1.3*	17.9 ± 0.9	27.5 ± 1.3*
Pg	39.5 ± 3.0*	21.7 ± 0.9	25.5 ± 0.9*

Values represent percentage of cells in the various stages of the cell cycle. Data represent the mean ± SEM of 3 individual experiments
*$P < 0.05$ compared with ethanol (EtOH) control.

$\times 10^5$ CPM/mg protein, $P < .0001$) increased FDG uptake in T47D YB cells compared with ethanol ($5.5 \pm 0.8 \times 10^5$ CPM/mg protein). PR protein expression in T47D YA and YB cells were also measured (Fig. 4B). T47D YA cells had higher levels of PR protein than T47D YB cells (1.0 ± 0.3 vs 0.2 ± 0.1, respectively, $P = .04$). Additionally, PR transcriptional activity was measured in T47D YA and YB cells that were hormone deprived and then treated with 10 nM PR agonists for 24 hours (Fig. 4C and 4D). R5020, MPA, and MA caused a significant increase in PR-A transcriptional activation compared with ethanol control in T47D YA cells (81.6 ± 10.5 fold change, $P < .0001$; 65.1 ± 4.8 fold change, $P = .0005$; and 64.9 ± 12.5 fold change, $P = .0005$ vs 1.0 ± 0.2, relatively). PR-B transcriptional activation was also increased in T47D YB cells after R5020 (2772 ± 150.4 fold change, $P = 0.0001$), MPA (1618 ± 61.4 fold change, $P = .007$), and MA (1843 ± 465.3 fold change, $P = 0.003$) compared with ethanol control (1.0 ± 0.1). Thus, either PR isoform can increase FDG uptake in T47D cells treated with PR agonists.

PR Antagonists Mitigate R5020-Mediated Increase in FDG Uptake

To further investigate the role ligand-activated PR plays in mediating FDG uptake, the antagonists mifepristone (RU486) [52, 53] and ulipristal acetate (UPA; CBD-2914) [54] were used to pharmacologically inhibit PR transcriptional activity. T47D cells were treated with either 100 nM RU486 or UPA in the presence of 1 nM R5020 for 24 hours. Both RU486 and UPA inhibited R5020-mediated increase in FDG uptake compared with R5020 alone ($7.6 \pm 0.4 \times 10^5$ CPM/mg protein, $7.3 \pm 0.3 \times 10^5$ CPM/mg protein vs $12.7 \pm 0.8 \times 10^5$ CPM/mg protein, respectively, Fig. 5A). Inhibition of PR transcriptional activity by these antagonists was confirmed using a reporter gene assay (Fig. 5B). Thus, pharmacologic of inhibition of PR transcriptional activity mitigates R5020-mediated increase in FDG uptake.

PR Expression Is Required for Increased FDG Uptake After R5020 Treatment

Since pharmacologic inhibition of PR prevents FDG uptake after R5020 treatment, the direct role of PR was evaluated by using T47D PR KO cells and their scrambled control (T47D Scr) [41]. First, PR KO was confirmed by Western blot which showed T47D PR KO cells had no detectable PR-B or PR-A protein (Fig. 6A). To confirm PR transcriptional activity, T47D WT, Scr, and PR KO cells were treated with either ethanol control or 10 nM R5020 for 24 hours and PR transactivation was measured using a reporter gene assay (Fig. 6B). There was a significant increase in PR transcriptional activity after R5020 treatment compared with ethanol in T47D WT (2.2 ± 0.06 vs 0.0004 ± 0.00002, $P < .0001$) and T47D Scr cells (2.7 ± 0.1 vs 0.0008 ± 0.0002, $P < .0001$). However, the PR KO cells demonstrated no increase in transcriptional activity in response to R5020. Additionally, the PR-regulated endogenous target gene [7, 55], *FKBP5* (FK506 binding protein 5) mRNA expression was measured to confirm PR KO (Fig. 6C). Cells were hormone deprived for 3 days and then treated with 10 nM R5020 for 12 and 24 hours. T47D WT cells had an increase in *FKBP5* expression at 12 hours (51.3 ± 0.2 fold change; $P < .0001$) and at 24 hours (29.6 ± 0.2 fold change; $P < .0001$) compared with ethanol. Similarly, T47D Scr cells had a significant increase in *FKBP5* at 12 hours (67.4 ± 0.7 fold change; $P < .0001$) and at 24 hours (41.4 ± 0.2 fold change; $P < .0001$). T47D PR KO cells had no measurable *FKBP5* expression. To determine if PR is directly responsible for PR agonists increasing FDG uptake, these cells were treated with 100 nM R5020, MPA, or MA for 24 hours (Fig. 6D). In T47D PR KO cells,

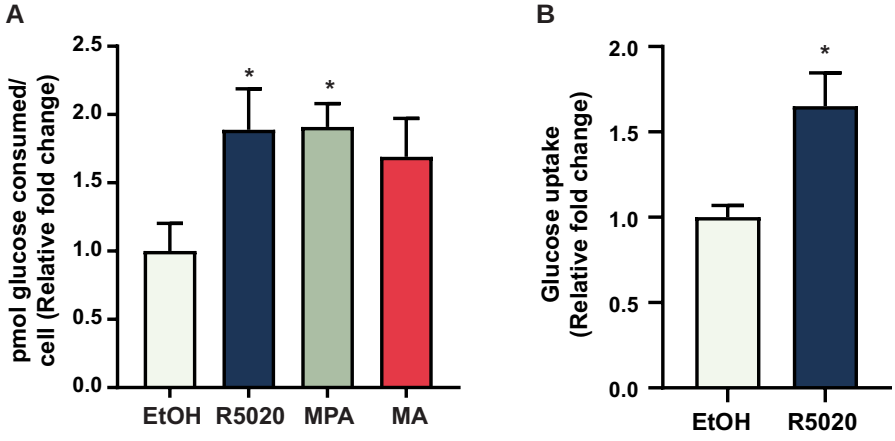

Figure 2. PR agonist induction of glucose uptake in T47D cells. T47D cells were steroid hormone deprived for 3 days then treated with 100 nM of R5020, MPA, or MA, or ethanol control for 24 hours. (A) Glucose consumption was measured in T47D cells using a glucometer. (B) 2-deoxyglucose uptake was measured in T47D cells using the Glucose Uptake-Glo assay. Values were normalized to the ethanol control. Data represent the mean ± SEM of 3 independent experiments. *$P < .05$ compared with ethanol.

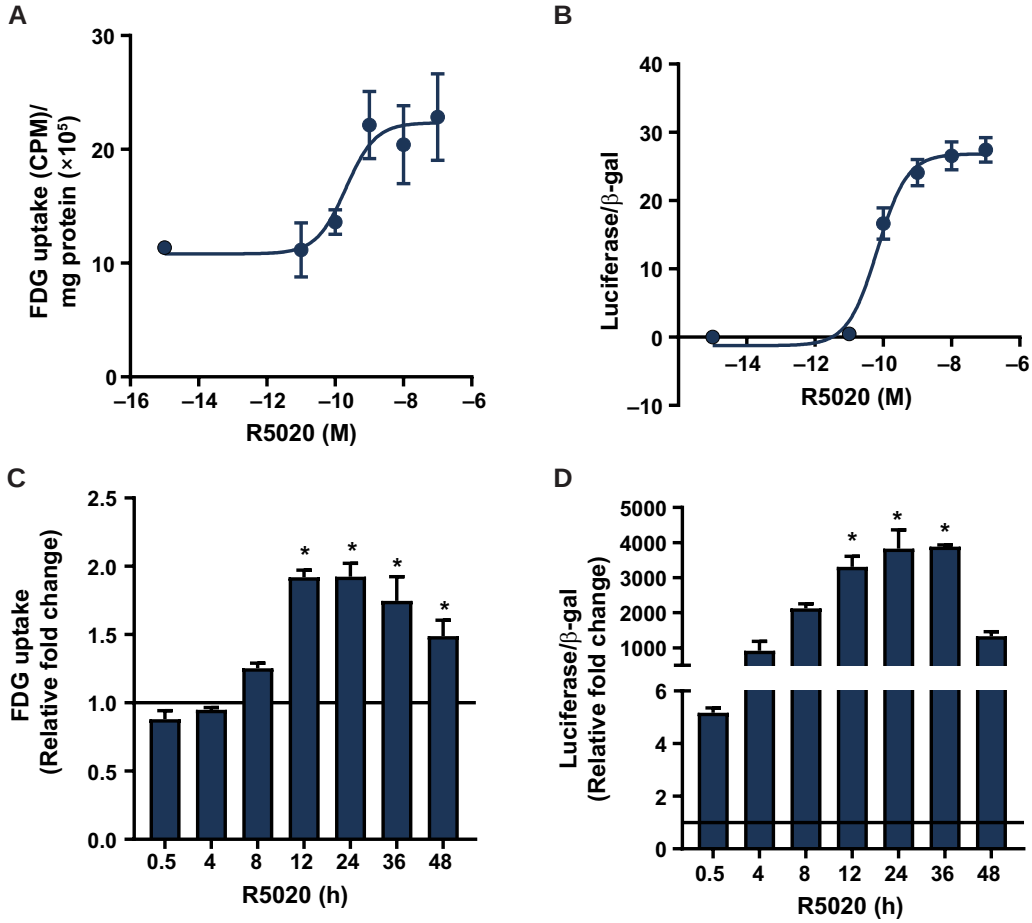

Figure 3. Dose titration and time course of FDG uptake and PR transcriptional activation in response to R5020. T47D cells were steroid hormone deprived for 3 days prior to experimentation. Cells were seeded and treated with increasing doses of R5020 (0.01-100 nM) for 24 hours and (A) FDG uptake and (B) reporter gene assays for PR transcriptional activation were performed. Cells were treated with 100 nM R5020 for varying times (0.5-48 hours) and data normalized to the ethanol control. (C) FDG uptake assay and (D) reporter gene assay for PR transcriptional activation were performed. Data represent the mean ± SEM of 3 independent experiments. *$P < .05$ compared with ethanol.

FDG uptake did not increase after treatment with R5020, MPA, or MA (0.83 ± 0.14 fold, 0.98 ± 0.12 fold, or 1.0 ± 0.08 fold, respectively). For comparison, treating the T47D Scr cells with R5020, MPA, or MA increased FDG uptake by 2.02 ± 0.11 fold ($P = .0002$), 1.88 ± 0.10 fold ($P = .0006$), and 1.84 ± 0.13 fold ($P = .0008$) compared with ethanol control, which was similar to T47D WT. Taken together, these data suggest that PR is essential for mediating increased FDG uptake in T47D cells.

Transcription and Translation Are Required for Ligand-Activated PR Induction of FDG Uptake

To investigate whether new RNA and protein synthesis are required for PR agonist–induced FDG uptake, the inhibitors actinomycin D and cycloheximide were used, respectively. Actinomycin D binds to DNA and inhibits RNA polymerase elongation thereby preventing RNA synthesis. Cycloheximide inhibits protein synthesis by preventing translational elongation. T47D cells were pretreated with actinomycin D (1 μM) or cycloheximide (10 μg/mL) for 1 hour prior to the addition of 100 nM R5020. FDG uptake was measured after 24 hours treatment (Fig. 7A). Both actinomycin D and cycloheximide were able to inhibit R5020-induced FDG uptake ($P = .85$ and $P = .65$, respectively). Thus, ligand-activated PR induction of FDG uptake requires both transcription and new protein synthesis.

R5020 Treatment Increases Expression and Activity of Proteins Involved in Glucose Uptake, Glycolysis, and Pentose Phosphate Pathway

T47D WT, Scr, and PR KO cells were hormone deprived for 3 days, then treated with 10 nM R5020 for 12 and 24 hours and mRNA was measured for selected candidate genes involved in glucose uptake, glycolysis, and the pentose phosphate pathway (Fig. 7B-D). After 12 hours of treatment, there was a significant increase in *GLUT1* and *PFKFB3* mRNA expression compared with ethanol in T47D WT cells (3.5 ± 0.4, $P < .0001$ and a 4.7 ± 0.7, $P < .0001$, respectively). *GLUT1* mRNA expression remained increased at 24 hours with a 2.2 ± 0.4 fold change ($P = .01$). *GLUT4* expression was also significantly increased at 24 hours (2.2 ± 0.7, $P = .009$). There was no significant change in expression of *GLUT12* or *HK2*. For T47D Scr cells, R5020 significantly increased *GLUT1* expression at 12 hours (3.0 ± 0.5, $P = .0012$) and *PFKFB3* expression at 12 and 24 hours (8.3 ± 0.9, $P < .0001$ and 4.6 ± 0.8, $P < .0001$, respectively). However, there

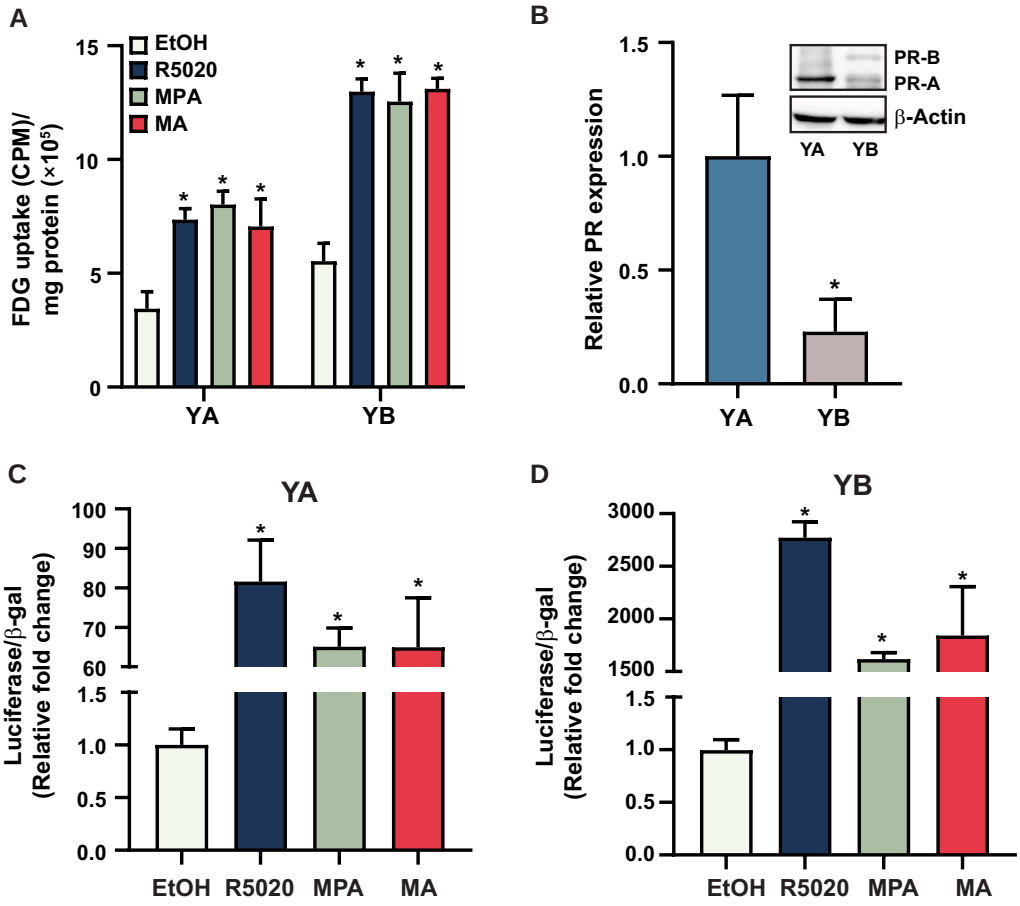

Figure 4. PR-A and PR-B isoforms increase FDG uptake after agonist treatment. T47D YA and YB cells were steroid hormone deprived for 3 days, seeded, and the next day treated with 100 nM R5020, MPA, MA, or ethanol control for 24 hours. (A) FDG uptake assay was performed and PR protein expression was measured by Western blot analysis (B) in T47D YA and YB cells. Values in B were normalized to the actin loading control then to T47D YA PR expression. PR transcriptional activation was confirmed with a reporter gene assay for T47D YA (C) and T47D YB (D) cells. Data represent the mean ± SEM of 3 independent experiments. *$P < .05$ compared with ethanol in (A), (C), and (D) or YA in (B).

was no significant increase in mRNA expression of these genes in T47D PR KO cells.

PR binding sites in the presence of R5020 in T47D cells near these genes were identified using a published ChIP sequencing (ChIP-Seq) data set (GEO accession number GSE68359) [35] (Table 2). *GLUT1*, *PFKFB3*, *G6PD*, and *6PGD* all have PR binding sites containing a full PRE located within 100 kb of their respective transcription start sites, suggesting that these

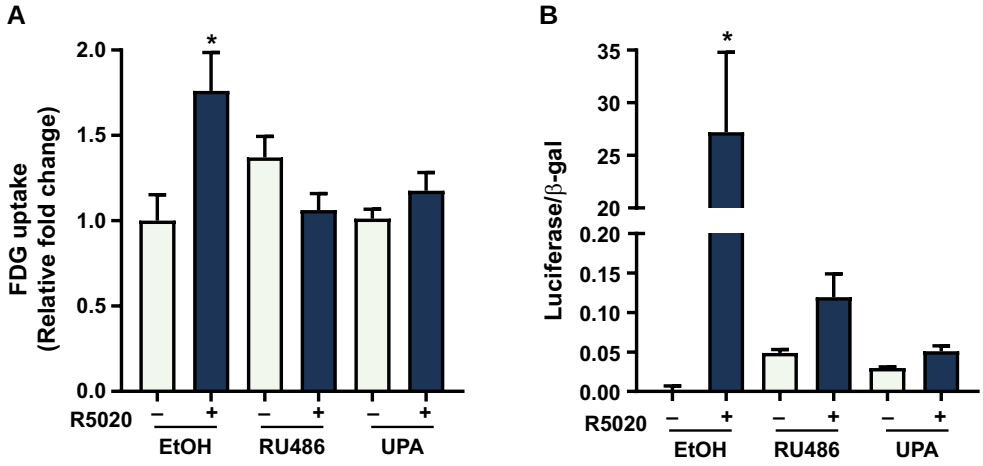

Figure 5. Pharmacologic inhibition of PR transcriptional activity prevents R5020-mediated FDG uptake. T47D cells were steroid hormone deprived for 3 days prior to experimentation. Cells were seeded, then cotreated for 24 hours with 100 nM mifepristone (RU486) or ulipristal acetate (UPA) in the presence or absence of 10 nM R5020. (A) FDG uptake and (B) reporter gene assays for PR transcriptional activation were performed. FDG uptake is normalized to ethanol treated cells. Data represents the mean ± SEM of 3 independent experiments. *$P < .05$ compared with ethanol.

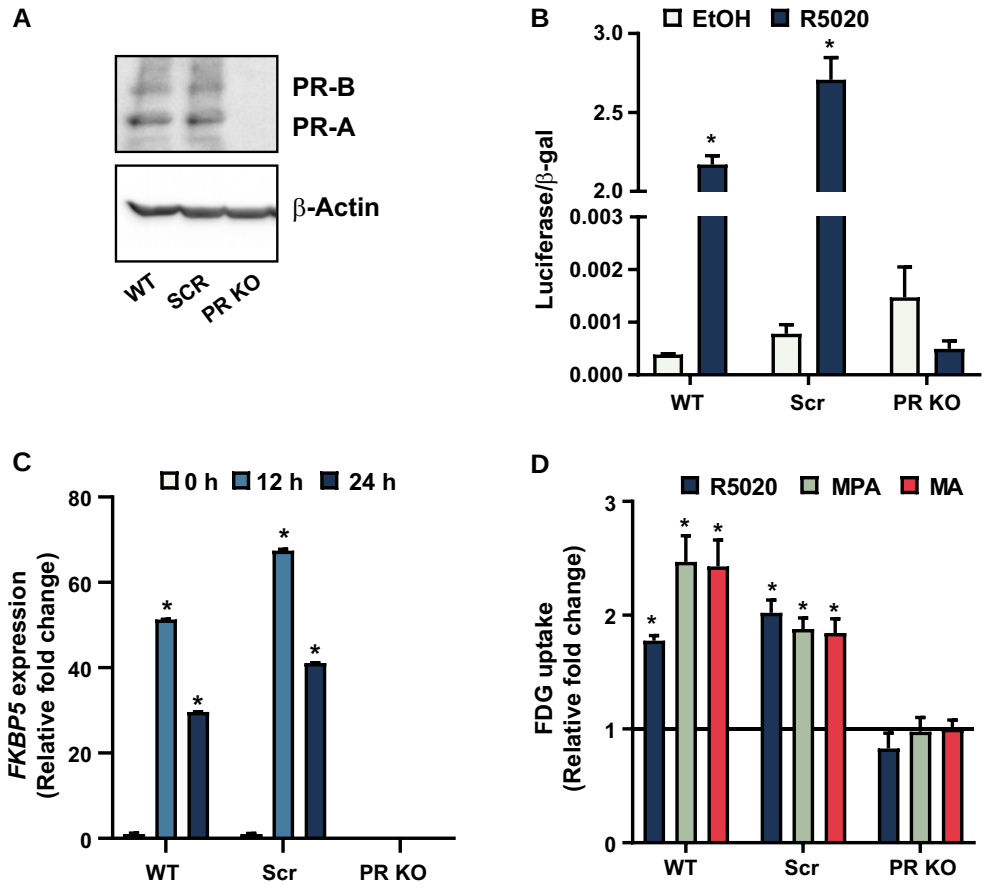

Figure 6. Genetic knockout of PR inhibits R5020-mediated FDG uptake. PR protein expression in T47D cells with CRISPR/Cas9 *PGR* gene knockout (PR KO), their scrambled control (Scr), and wild-type (WT) was confirmed with Western blot analysis (A). Transcriptional activation after 24 hours treatment with 10 nM R5020 or ethanol vehicle control (EtOH) was determined using a reporter gene assay (B) and measurement of an endogenous PR-regulated gene, *FKBP5*, via qPCR (C). Cells were steroid hormone deprived for 3 days and treated with 100 nM R5020, MPA, MA, or ethanol vehicle for 24 hours and (D) FDG uptake was performed. Data is normalized to ethanol control and expressed as relative fold change. Data represent the mean ± SEM of 3 independent assays for B and D. Data represent the mean ± SD for C. *$P < .05$ compared with ethanol.

genes may be directly regulated by PR in response to R5020. For confirmation, ChIP-qPCR was performed focusing on the PR binding sites upstream of the *GLUT1* and *PFKFB3* genes identified from the published ChIP-Seq data set. *SYNE1* was used as a negative control for PR binding. There was a significant increase in PR protein binding to the *SLC2A1 (GLUT1)* and *PFKFB3* genes in response to R5020 treatment (Fig. 7E and 7F).

Additionally, the activity of G6PD and 6PGD, two enzymes in the pentose phosphate pathway, were measured. R5020 treatment significantly increased G6PD activity compared with ethanol (50.4 ± 1.6 vs 39.4 ± 1.6 mU/protein, $P = .007$; Table 3). 6PGD activity was also significantly increased in T47D cells after R5020 treatment (6.3 ± 0.08 vs 4.5 ± 0.5 mU/protein, $P = .02$; Table 3). Taken together, R5020 affected the expression and activity of proteins involved in glucose uptake, glycolysis, and the pentose phosphate pathway.

Discussion

The purpose of this study was to evaluate the role of PR in regulating glucose and FDG uptake in breast cancer cells with the future translational goal of using FDG PET imaging for predicting and assessing early response to new PR-targeted endocrine therapy agents in clinical trials. This study focused on T47D breast cancer cells since they express high levels of PR protein and allow the study of PR function in an estrogen-free system, which is important given the independent, confounding effects of estrogen on glycolysis and FDG uptake [56–59]. We report that progesterone and progestins increase FDG uptake in T47D cells, which can be inhibited by pharmacologic antagonists of PR transcriptional activity. Progestin-stimulated FDG uptake is dose dependent (half maximal effective concentration 0.2 nM), requires at least 12 hours of treatment for effect, can be mediated by either PR-B or PR-A, and requires both transcription and translation. Despite lower PR-B expression than PR-A in the cell model used, there was a stronger impact on FDG uptake in PR-B–expressing cells. This phenomenon could be attributed to PR-B being a stronger transactivator than PR-A [4–6]. Progestin-stimulated FDG uptake is independent of GR signaling since treatment with dexamethasone, a GR selective agonist, showed no effect. Additionally, R5020 increased the mRNA expression of *GLUT1* and *PFKFB3* in T47D WT and Scr cells but not in PR KO cells. PRE sites were identified for both *GLUT1* and *PFKFB3* suggesting direct transcriptional regulation, which is supported by ChIP-qPCR results confirming PR binding. T47D WT cells also had an increase in G6PD and 6PGD enzymatic activity within the pentose phosphate pathway. Together, these findings support a classic genomic

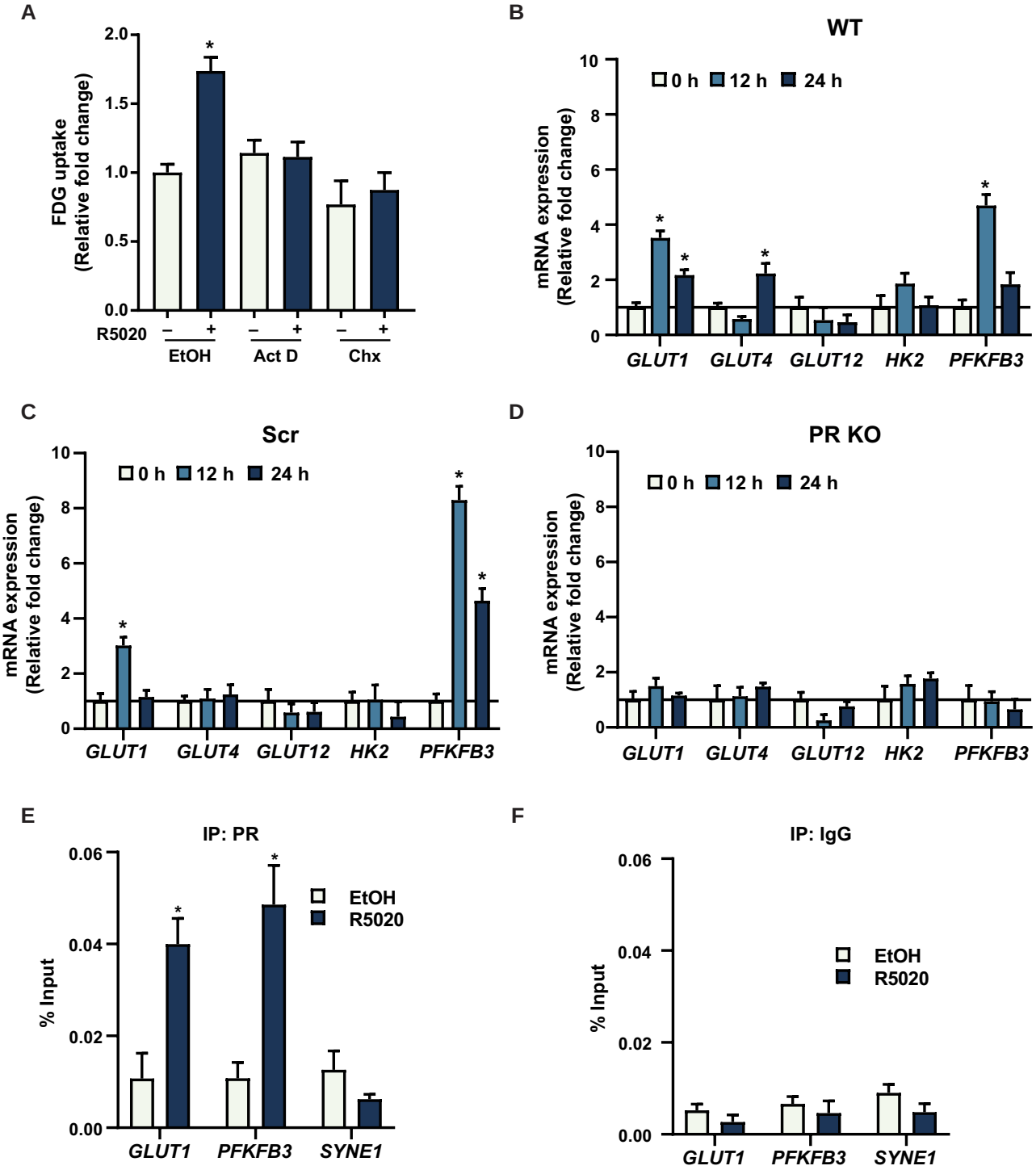

Figure 7. Progestin-stimulated gene expression and enzymatic activity of proteins involved in glucose uptake, glycolysis, and the pentose phosphate pathway. T47D cells were steroid hormone deprived for 3 days. (A) Cells were pretreated with 1 μM actinomycin D (Act D) or 10 μg/mL cycloheximide (Chx) for 1 hour and then treated with 100 nM R5020 for 24 hours. FDG uptake was measured and normalized to protein. Data were normalized to vehicle control. T47D WT (B), Scr (C), and PR KO (D) cells were treated with 100 nM R5020 for 12 and 24 hours. Data were normalized to *RPLP0*, a housekeeping gene, then normalized to each ethanol vehicle control (0 hours). ChIP-qPCR was performed on T47D cells treated for 3 hours with 100 nM R5020 or ethanol control using (E) PR antibody or (F) rabbit immunoglobulin (IgG). Data represents the mean ± SEM of 3 independent assays for A, E, and F. Data represents the mean ± SD for B, C, and D. **P* < .05 compared with ethanol.

PR signaling mechanism that mediates progesterone and progestin stimulated FDG uptake (Fig. 8).

The results of our study expand upon previous work initially reporting an effect of progesterone on GLUTs. In the study by Medina et al, progesterone treatment of ZR-75-1 breast cancer cells increased *GLUT1* mRNA and protein, *GLUT3* mRNA and protein, and GLUT4 protein [60]. *GLUT2* mRNA and protein expression were unaffected by progesterone treatment [60]. The direct mechanistic role for PR was not explored in this prior study. Our results also demonstrate an

Table 2. PR binding sites near selected genes in the presence of R5020 for T47D cells

Gene	Full PRE (distance to TSS)	Half PRE (distance to TSS)	No PRE
SLC2A1 (GLUT1)	−72 605, −33 300, +11 624, +12 483, +20 008	−2062, +7764, +21 169, +26 266, +27 031, +98 711	None
SLC2A4 (GLUT4)	None	None	None
SLC2A12 (GLUT12)	−50 554	−64 838, −57 179, +3369, +45 402	None
HK2	−72 418, +11 503	None	+32 638
PFKFB3	+26 654, +45 996, +54 553, +94 351	−31 266, −29 290, −26 683, +23 304, +30 665, +51 066, +52 987	None
G6PD	−5005	+4101	None
6PGD	−10 666, +29 900	None	None

The locations of PR binding sites following treatment with R5020 that are within 100 kb of the TSS of selected genes. The presence of a half-PRE (RGnACA or TGTnCY) or full-PRE (RGnACAnrnTGTnCY) sequence in the binding sites is noted. Data were obtained from a previously published dataset using T47D cells (GEO accession number GSE68359 [35]).
Abbreviations: *6PGD*, 6-phosphogluconate dehydrogenase; *G6PD*, glucose-6-phosphate dehydrogenase; *HK2*, hexokinase 2; *PFKFB3*, 6-phosphofructo-2-kinase/fructose-2,6-biphosphatase 3; PRE, progesterone receptor response element; TSS, transcription start site.

Table 3. G6PD and 6PGD enzymatic activity in T47D cells

	G6PD	6PGD
EtOH	37.8 ± 4.7	4.5 ± 0.5
R5020	47.8 ± 5.4*	6.3 ± 0.08*

Values are mU/protein. Data represent the mean ± SEM of 3 individual experiments.
*$P < 0.05$ compared with EtOH control.
Abbreviations: 6PGD = 6-phosphogluconate dehydrogenase; G6PD, glucose-6-phosphate dehydrogenase; EtOH, ethanol.

increase in *GLUT1* mRNA by progestin treatment using T47D cells and expand existing knowledge by demonstrating a classic genomic PR-signaling mechanism that mediates FDG uptake in part through increased *GLUT1* expression. Overexpression of *GLUT1* is common in breast cancer [17, 20, 61–63] and correlates positively with FDG uptake [64]. Furthermore, *GLUT1* expression has been associated with higher tumor grade [65–67] and reduced patient survival, thus a poor prognostic factor [67–69].

In addition to stimulation of *GLUT1* mRNA expression, the results from our study demonstrated an increase in *PFKFB3* mRNA expression in response to R5020 treatment in T47D cells. PFKFB3 is a key regulator of glycolysis and is one of four isoenzymes responsible for catalyzing and degrading fructose 2,6-bisphosphate [70]. Fructose 2,6-bisphosphate is an activator of 6-phosphofructo-1-kinase (PFK-1), the most important regulatory enzyme for glycolysis [71, 72]. PFKFB3 has been shown to have a higher kinase to phosphatase ratio that favors glycolytic flux [73]. In addition to promoting glycolysis, PFKFB3 also promotes cell cycle progression, survival, angiogenesis, immunosuppression, and metastasis in cancer [74–77]. Our results agree with previous studies demonstrating that treatment of T47D and MCF-7 cells with the synthetic progestins ORG2058 or norgestrel increased expression of *PFKFB3*, which was inhibited by the PR antagonist mifepristone [70, 78]. In the study by Novellasdemunt et al, chromatin immunoprecipitation experiments demonstrated recruitment of PR to the DNA region flanking a partial PRE sequence within the *PFKFB3* promoter in response to R5020 treatment in T47D cells supporting a classic genomic PR signaling mechanism [78]. The authors also demonstrated rapid, nongenomic progestin signaling through the ERK (extracellular signal–regulated kinase)/RSK (ribosomal S6 kinase) pathway resulting in phosphorylation of PFKFB3 protein and increased enzymatic activity as a dual mechanism for progestin activation of glycolysis in breast cancer cells [78]. A recently published study also showed that progestin treatment shifts metabolism towards glycolysis in T47D cells and a patient-derived cell line, UCD65, which are highly PR-positive [79], consistent with our findings with FDG uptake.

The results of our study also demonstrated that ligand-activated PR increases the enzymatic activity of G6PD and 6PGD within the pentose phosphate pathway, an important pathway in cancer cell metabolism. G6PD is the rate-limiting enzyme for the pentose phosphate pathway, which produces ribose 5-phosphate, for nucleotide biosynthesis, and NADPH, for biosynthesis of fatty acids and for redox homeostasis [80–82]. Upregulation of G6PD expression or enzymatic activity is a common phenotype in many malignancies including breast cancer and may be associated with poor prognosis and endocrine resistance [80, 83, 84]. Our results using T47D breast cancer cells agree with previous studies using MCF-7 breast cancer cells demonstrating that the PR agonist R5020 increases G6PD activity [85] and is inhibited by the antagonist, RU486 [86]. In addition, a PR binding site with a PRE sequence can be found upstream of the *G6PD* transcription start site in T47D cells treated with R5020 (Table 1).

This work focused on upstream proteins involved in glucose metabolism that could impact FDG uptake and retention for potential clinical translation. FDG PET imaging is FDA approved for clinical use and increased FDG uptake in response to brief treatment with estradiol or tamoxifen (ie, metabolic flare) in patients with advanced breast cancer has been shown to be associated with clinical response to ER-targeted endocrine therapy agents [87–90]. Given the role for PR regulation in glucose uptake, metabolic imaging with FDG PET could be similarly investigated for assessing early treatment response to new anti-progestins in clinical development.

A different type of metabolic imaging uses hyperpolarized carbon-13 (^{13}C) magnetic resonance imaging (MRI), which largely focuses on lactate production from hyperpolarized [1-^{13}C]-pyruvate occurring further downstream from glucose influx and phosphorylation by hexokinase [91]. Pyruvate is the final product of glycolysis and is converted to lactate by the enzyme lactate dehydrogenase (LDH). Dynamic hyperpolarized ^{13}C MRI can be used to visualize and quantify apparent LDH activity via the pyruvate to lactate conversion rate (k_{PL}) [91]. Increased LDH activity in T47D and MCF-7 breast cancer cells treated with R5020 has been demonstrated, which is likely mediated via classic genomic PR functional activity since the effect was inhibited by RU486 and by inhibitors of transcription and translation [92–95]. Thus, hyperpolarized ^{13}C MRI may represent another potential noninvasive imaging approach for assessing in vivo PR functional activity in breast cancer.

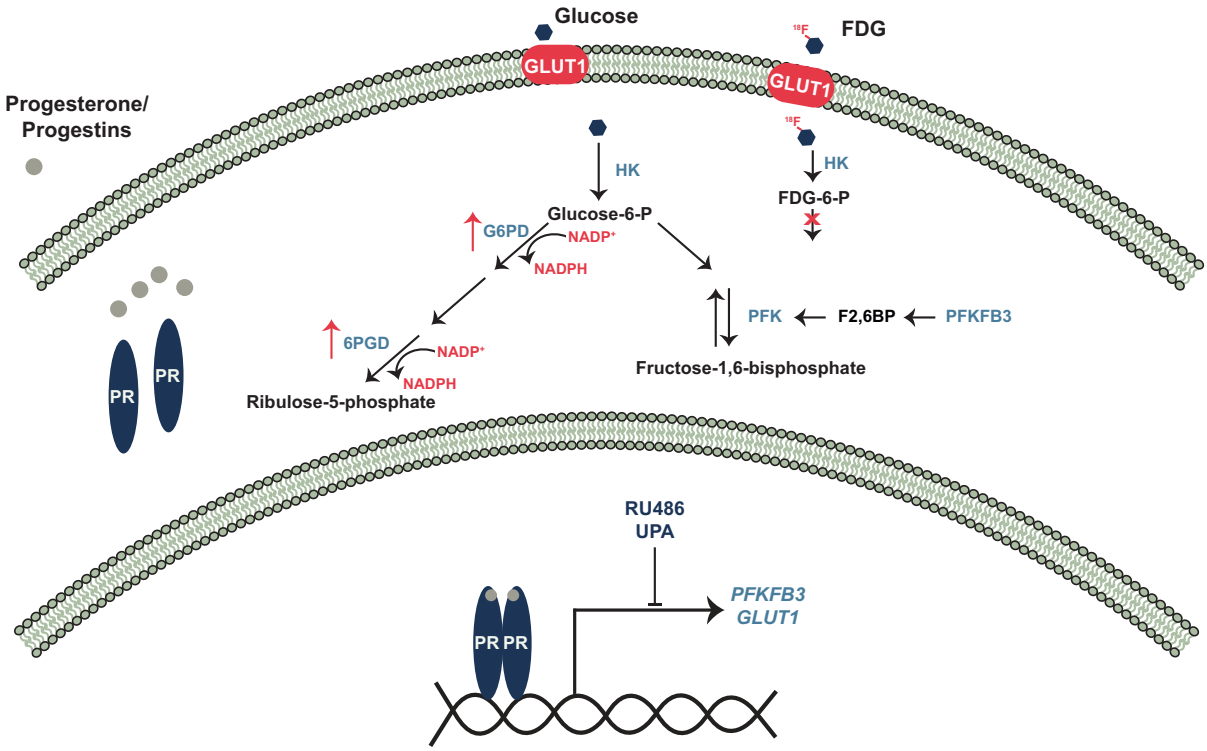

Figure 8. Proposed model for PR regulation of glucose and FDG uptake in T47D breast cancer cells. Progesterone receptor (PR) is activated by progesterone and progestins which promotes transcription of *GLUT1* and *PFKB3*, increased glucose transport into the cell via GLUT1, and increased glycolysis through PFKFB3. Activated PR also increases glucose-6-phosphate-dehydrogenase (G6PD) and 6-phosphogluconate dehydrogenase (6PGD) enzymatic activity which promotes increased glucose uptake. ^{18}F-fluorodeoxyglucose (FDG) is transported into the cell via GLUT1 and is then phosphorylated by hexokinase [39]. Phosphorylated-FDG is not processed further leading to accumulation of FDG within the cell. Phosphofructokinase (PFK), 6-phosphofructo-2-kinase/fructose-2,6-biphosphatase 3 (PFKFB3), mifepristone (RU486), and ulipristal acetate (UPA).

Hyperpolarized ^{13}C MRI of pyruvate metabolism to lactate has been demonstrated in preclinical rodent models of breast cancer and may enable early detection of treatment response and resistance [96–99]. Although still investigational and not widely available, recent pilot studies have demonstrated safety and feasibility of translating hyperpolarized ^{13}C MRI for measuring pyruvate metabolism to patients with early-stage breast cancer [100, 101]. With combined PET/MRI scanners now available and validated for breast cancer imaging [102, 103], simultaneous characterization of PR regulation of upstream glucose uptake and hexokinase activity with FDG and downstream regulation of LDH activity via hyperpolarized ^{13}C MRI is technically possible.

Collectively, the results of this study suggest that monitoring alterations in FDG uptake and trapping via progestin stimulation or antiprogestin inhibition could provide insight into PR function in breast cancer. These findings provide the rationale for subsequent in vivo testing using tumor xenografts and small animal FDG PET imaging. In conclusion, progesterone and progestins increase FDG uptake in T47D breast cancer cells through the classical action of PR as a ligand-activated transcription factor. Ligand-activated PR ultimately increases expression and activity of proteins involved in glucose uptake, glycolysis, and the pentose phosphate pathway.

Acknowledgments

We thank Dr. Julie Kim (Northwestern University), Dr. Kathryn Horwitz (University of Colorado), and Dr. Carol Lange (University of Minnesota) for permitting access to cell lines. We also thank Dr. Michael L. McCormick for performing the G6PD and 6PGD assay at the University of Iowa Free Radical and Radiation core.

Funding

University of Wisconsin Carbone Cancer Center Support Grant P30 CA014520 and the Department of Radiology, University of Wisconsin School of Medicine and Public Health. This work was partially funded by an NIH R01 grant to ETA (CA260140). Funding sources for AMF include the American Cancer Society (RSG-22-015-01-CCB) and the National Cancer Institute (R01 CA272571).

Disclosures

K.S., R.M.R., and E.T.A. have nothing to declare. A.M.F. receives book chapter royalty from Elsevier, Inc. and has served on an advisory board for GE Healthcare. The Department of Radiology receives research support from GE Healthcare.

Data Availability

Original data generated and analyzed during this study are included in this published article or in the data repositories listed in References.

References

1. Hwang KT, Kim J, Jung J, *et al.* Impact of breast cancer subtypes on prognosis of women with operable invasive breast cancer: a

population-based study using SEER database. *Clin Cancer Res*. 2019;25(6):1970-1979.
2. Blamey RW, Hornmark-Stenstam B, Ball G, *et al.* ONCOPOOL—a European database for 16,944 cases of breast cancer. *Eur J Cancer*. 2010;46(1):56-71.
3. Kastner P, Krust A, Turcotte B, *et al.* Two distinct estrogen-regulated promoters generate transcripts encoding the two functionally different human progesterone receptor forms A and B. *EMBO J*. 1990;9(5):1603-1614.
4. Vegeto E, Shahbaz MM, Wen DX, Goldman ME, O'Malley BW, McDonnell DP. Human progesterone receptor A form is a cell- and promoter-specific repressor of human progesterone receptor B function. *Mol Endocrinol*. 1993;7(10):1244-1255.
5. Salem K, Kumar M, Yan Y, *et al.* Sensitivity and isoform specificity of (18)F-fluorofuranylnorprogesterone for measuring progesterone receptor protein response to estradiol challenge in breast cancer. *J Nucl Med*. 2019;60(2):220-226.
6. Giangrande PH, Pollio G, McDonnell DP. Mapping and characterization of the functional domains responsible for the differential activity of the A and B isoforms of the human progesterone receptor. *J Biol Chem*. 1997;272(52):32889-32900.
7. Richer JK, Jacobsen BM, Manning NG, Abel MG, Wolf DM, Horwitz KB. Differential gene regulation by the two progesterone receptor isoforms in human breast cancer cells. *J Biol Chem*. 2002;277(7):5209-5218.
8. Lange CA. Integration of progesterone receptor action with rapid signaling events in breast cancer models. *J Steroid Biochem Mol Biol*. 2008;108(3-5):203-212.
9. Pedroza DA, Subramani R, Lakshmanaswamy R. Classical and non-classical progesterone signaling in breast cancers. *Cancers (Basel)*. 2020;12(9):2440.
10. Blundon MA, Dasgupta S. Metabolic dysregulation controls endocrine therapy-resistant cancer recurrence and metastasis. *Endocrinology*. 2019;160(8):1811-1820.
11. Warburg O. On the origin of cancer cells. *Science*. 1956; 123(3191):309-314.
12. Warburg O. On respiratory impairment in cancer cells. *Science*. 1956;124(3215):269-270.
13. Thorne JL, Campbell MJ. Nuclear receptors and the Warburg effect in cancer. *Int J Cancer*. 2015;137(7):1519-1527.
14. Heiden MG V, Cantley LC, Thompson CB. Understanding the Warburg effect: the metabolic requirements of cell proliferation. *Science*. 2009;324(5930):1029-1033.
15. Hanahan D, Weinberg RA. Hallmarks of cancer: the next generation. *Cell*. 2011;144(5):646-674.
16. Salas JR, Clark PM. Signaling pathways that drive (18)F-FDG accumulation in cancer. *J Nucl Med*. 2022;63(5):659-663.
17. Barbosa AM, Martel F. Targeting glucose transporters for breast cancer therapy: the effect of natural and synthetic compounds. *Cancers (Basel)*. 2020;12(1):154.
18. Nualart F, Los Angeles Garcia M, Medina RA, Owen GI. Glucose transporters in sex steroid hormone related cancer. *Curr Vasc Pharmacol*. 2009;7(4):534-548.
19. Macheda ML, Rogers S, Best JD. Molecular and cellular regulation of glucose transporter (GLUT) proteins in cancer. *J Cell Physiol*. 2005;202(3):654-662.
20. Medina RA, Owen GI. Glucose transporters: expression, regulation and cancer. *Biol Res*. 2002;35(1):9-26.
21. Pauwels EK, Sturm EJ, Bombardieri E, Cleton FJ, Stokkel MP. Positron-emission tomography with [18F]fluorodeoxyglucose. Part I. Biochemical uptake mechanism and its implication for clinical studies. *J Cancer Res Clin Oncol*. 2000;126(10):549-559.
22. Smith TA. The rate-limiting step for tumor [18F] fluoro-2-deoxy-D-glucose (FDG) incorporation. *Nucl Med Biol*. 2001;28(1):1-4.
23. Caracó C, Aloj L, Chen LY, Chou JY, Eckelman WC. Cellular release of [18F]2-fluoro-2-deoxyglucose as a function of the glucose-6-phosphatase enzyme system. *J Biol Chem*. 2000; 275(24):18489-18494.
24. Fowler AM, Cho SY. PET Imaging for breast cancer. *Radiol Clin North Am*. 2021;59(5):725-735.
25. Vranjesevic D, Schiepers C, Silverman DH, *et al.* Relationship between 18F-FDG uptake and breast density in women with Normal breast tissue. *J Nucl Med*. 2003;44(8):1238-1242.
26. Lakhani P, Maidment AD, Weinstein SP, Kung JW, Alavi A. Correlation between quantified breast densities from digital mammography and 18F-FDG PET uptake. *Breast J*. 2009;15(4): 339-347.
27. Koo HR, Moon WK, Chun IK, *et al.* Background (18)F-FDG uptake in positron emission mammography (PEM): correlation with mammographic density and background parenchymal enhancement in breast MRI. *Eur J Radiol*. 2013;82(10):1738-1742.
28. Shimizu Y, Satake H, Ishigaki S, *et al.* Physiological background parenchymal uptake of (18)F-FDG in normal breast tissues using dedicated breast PET: correlation with mammographic breast composition, menopausal status, and menstrual cycle. *Ann Nucl Med*. 2022;36(8):728-735.
29. Jung Y, Kim TH, Kim JY, Han S, An YS. The effect of sex hormones on normal breast tissue metabolism: evaluation by FDG PET/CT. *Medicine (Baltimore)*. 2019;98(27):e16306.
30. Lin CY, Ding HJ, Liu CS, Chen YK, Lin CC, Kao CH. Correlation between the intensity of breast FDG uptake and menstrual cycle. *Acad Radiol*. 2007;14(8):940-944.
31. Park HH, Shin JY, Lee JY, *et al.* Discussion on the alteration of 18F-FDG uptake by the breast according to the menstrual cycle in PET imaging. *Annu Int Conf IEEE Eng Med Biol Soc*. 2013;2013:2469-2472.
32. An YS, Jung Y, Kim JY, *et al.* Metabolic activity of normal glandular tissue on (18)F-fluorodeoxyglucose positron emission tomography/computed tomography: correlation with menstrual cycles and parenchymal enhancements. *J Breast Cancer*. 2017;20(4):386-392.
33. Miyake KK, Nakamoto Y, Saji S, *et al.* Impact of physiological hormonal fluctuations on (18)F-fluorodeoxyglucose uptake in breast cancer. *Breast Cancer Res Treat*. 2018;169(3):437-446.
34. Daniel AR, Gaviglio AL, Knutson TP, *et al.* Progesterone receptor-B enhances estrogen responsiveness of breast cancer cells via scaffolding PELP1- and estrogen receptor-containing transcription complexes. *Oncogene*. 2015;34(4):506-515.
35. Mohammed H, Russell IA, Stark R, *et al.* Progesterone receptor modulates ERalpha action in breast cancer. *Nature*. 2015; 523(7560):313-317.
36. Singhal H, Greene ME, Tarulli G, *et al.* Genomic agonism and phenotypic antagonism between estrogen and progesterone receptors in breast cancer. *Sci Adv*. 2016;2(6):e1501924.
37. Cottu PH, Bonneterre J, Varga A, *et al.* Phase I study of onapristone, a type I antiprogestin, in female patients with previously treated recurrent or metastatic progesterone receptor-expressing cancers. *PLoS One*. 2018;13(10):e0204973.
38. Lewis JH, Cottu PH, Lehr M, *et al.* Onapristone extended release: safety evaluation from phase I-II studies with an emphasis on hepatotoxicity. *Drug Saf*. 2020;43(10):1045-1055.
39. Lee O, Sullivan ME, Xu Y, *et al.* Selective progesterone receptor modulators in early-stage breast cancer: a randomized, placebo-controlled phase II window-of-opportunity trial using telapristone acetate. *Clin Cancer Res*. 2020;26(1):25-34.
40. Kamaraju S, Fowler AM, Weil E, *et al.* Leveraging antiprogestins in the treatment of metastatic breast cancer. *Endocrinology*. 2021;162(8):bqab060.
41. Davaadelger B, Murphy AR, Clare SE, Lee O, Khan SA, Kim JJ. Mechanism of telapristone acetate (CDB4124) on progesterone receptor action in breast cancer cells. *Endocrinology*. 2018;159-(10):3581-3595.
42. Sartorius CA, Groshong SD, Miller LA, *et al.* New T47D breast cancer cell lines for the independent study of progesterone B- and A-receptors: only antiprogestin-occupied B-receptors are switched to transcriptional agonists by cAMP. *Cancer Res*. 1994;54(14):3868-3877.

43. Strahle U, Klock G, Schutz G. A DNA sequence of 15 base pairs is sufficient to mediate both glucocorticoid and progesterone induction of gene expression. *Proc Natl Acad Sci U S A*. 1987;84(22):7871-7875.
44. MacGregor GR, Caskey CT. Construction of plasmids that express E. coli beta-galactosidase in mammalian cells. *Nucleic Acids Res*. 1989;17(6):2365.
45. Livak KJ, Schmittgen TD. Analysis of relative gene expression data using real-time quantitative PCR and the 2(−Delta Delta C(T)) method. *Methods*. 2001;25(4):402-408.
46. Langmead B, Salzberg SL. Fast gapped-read alignment with Bowtie 2. *Nat Methods*. 2012;9(4):357-359.
47. Zhang Y, Liu T, Meyer CA, *et al.* Model-based analysis of ChIP-Seq (MACS). *Genome Biol*. 2008;9(9):R137.
48. McLean CY, Bristor D, Hiller M, *et al.* GREAT Improves functional interpretation of cis-regulatory regions. *Nat Biotechnol*. 2010;28(5):495-501.
49. Grant CE, Bailey TL, Noble WS. FIMO: scanning for occurrences of a given motif. *Bioinformatics*. 2011;27(7):1017-1018.
50. Bailey TL, Boden M, Buske FA, *et al.* MEME SUITE: tools for motif discovery and searching. *Nucleic Acids Res*. 2009;37(Web Server issue):W202-W208.
51. Helzer KT, Szatkowski Ozers M, Meyer MB, *et al.* The phosphorylated estrogen receptor alpha (ER) cistrome identifies a subset of active enhancers enriched for direct ER-DNA binding and the transcription factor GRHL2. *Mol Cell Biol*. 2019;39(3):e00417-18.
52. Vegeto E, Allan GF, Schrader WT, Tsai MJ, McDonnell DP, O'Malley BW. The mechanism of RU486 antagonism is dependent on the conformation of the carboxy-terminal tail of the human progesterone receptor. *Cell*. 1992;69(4):703-713.
53. Raaijmakers HC, Versteegh JE, Uitdehaag JC. The X-ray structure of RU486 bound to the progesterone receptor in a destabilized agonistic conformation. *J Biol Chem*. 2009;284(29):19572-19579.
54. Attardi BJ, Burgenson J, Hild SA, Reel JR. In vitro antiprogestational/antiglucocorticoid activity and progestin and glucocorticoid receptor binding of the putative metabolites and synthetic derivatives of CDB-2914, CDB-4124, and mifepristone. *J Steroid Biochem Mol Biol*. 2004;88(3):277-288.
55. Magklara A, Smith CL. A composite intronic element directs dynamic binding of the progesterone receptor and GATA-2. *Mol Endocrinol*. 2009;23(1):61-73.
56. Rivenzon-Segal D, Boldin-Adamsky S, Seger D, Seger R, Degani H. Glycolysis and glucose transporter 1 as markers of response to hormonal therapy in breast cancer. *Int J Cancer*. 2003;107(2):177-182.
57. Imbert-Fernandez Y, Clem BF, O'Neal J, *et al.* Estradiol stimulates glucose metabolism via 6-phosphofructo-2-kinase (PFKFB3). *J Biol Chem*. 2014;289(13):9440-9448.
58. Garrido P, Morán J, Alonso A, González S, González C. 17β-estradiol activates glucose uptake via GLUT4 translocation and PI3K/akt signaling pathway in MCF-7 cells. *Endocrinology*. 2013;154(6):1979-1989.
59. Ko BH, Paik JY, Jung KH, Lee KH. 17beta-estradiol augments 18F-FDG uptake and glycolysis of T47D breast cancer cells via membrane-initiated rapid PI3K-Akt activation. *J Nucl Med*. 2010;51(11):1740-1747.
60. Medina RA, Meneses AM, Vera JC, *et al.* Estrogen and progesterone up-regulate glucose transporter expression in ZR-75-1 human breast cancer cells. *Endocrinology*. 2003;144(10):4527-4535.
61. Binder C, Binder L, Marx D, Schauer A, Hiddemann W. Deregulated simultaneous expression of multiple glucose transporter isoforms in malignant cells and tissues. *Anticancer Res*. 1997;17(6):4299-4304.
62. Brown RS, Wahl RL. Overexpression of Glut-1 glucose transporter in human breast cancer. An immunohistochemical study. *Cancer*. 1993;72(10):2979-2985.
63. Alexander CM, Martin JA, Oxman E, Kasza I, Senn KA, Dvinge H. Alternative splicing and cleavage of GLUT8. *Mol Cell Biol*. 2020;41(1):e00480-20.
64. Bos R, van Der Hoeven JJ, van Der Wall E, *et al.* Biologic correlates of (18)fluorodeoxyglucose uptake in human breast cancer measured by positron emission tomography. *J Clin Oncol*. 2002;20(2):379-387.
65. Alò PL, Visca P, Botti C, *et al.* Immunohistochemical expression of human erythrocyte glucose transporter and fatty acid synthase in infiltrating breast carcinomas and adjacent typical/atypical hyperplastic or normal breast tissue. *Am J Clin Pathol*. 2001;116(1):129-134.
66. Krzeslak A, Wojcik-Krowiranda K, Forma E, *et al.* Expression of GLUT1 and GLUT3 glucose transporters in endometrial and breast cancers. *Pathol Oncol Res*. 2012;18(3):721-728.
67. Deng Y, Zou J, Deng T, Liu J. Clinicopathological and prognostic significance of GLUT1 in breast cancer: a meta-analysis. *Medicine (Baltimore)*. 2018;97(48):e12961.
68. Zeng K, Ju GD, Wang H, Huang JS. GLUT1/3/4 As novel biomarkers for the prognosis of human breast cancer. *Transl Cancer Res*. 2020;9(4):2363-2377.
69. Wang J, Ye C, Chen C, *et al.* Glucose transporter GLUT1 expression and clinical outcome in solid tumors: a systematic review and meta-analysis. *Oncotarget*. 2017;8(10):16875-16886.
70. Hamilton JA, Callaghan MJ, Sutherland RL, Watts CK. Identification of PRG1, a novel progestin-responsive gene with sequence homology to 6-phosphofructo-2-kinase/fructose-2,6-bisphosphatase. *Mol Endocrinol*. 1997;11(4):490-502.
71. Van Schaftingen E. Fructose 2,6-bisphosphate. *Adv Enzymol Relat Areas Mol Biol*. 1987;59:315-395.
72. Rider MH, Bertrand L, Vertommen D, Michels PA, Rousseau GG, Hue L. 6-Phosphofructo-2-kinase/fructose-2,6-bisphosphatase: head-to-head with a bifunctional enzyme that controls glycolysis. *Biochem J*. 2004;381(Pt 3):561-579.
73. Sakakibara R, Kato M, Okamura N, *et al.* Characterization of a human placental fructose-6-phosphate, 2-kinase/fructose-2,6-bisphosphatase. *J Biochem*. 1997;122(1):122-128.
74. Yalcin A, Clem BF, Imbert-Fernandez Y, *et al.* 6-Phosphofructo-2-kinase (PFKFB3) promotes cell cycle progression and suppresses apoptosis via Cdk1-mediated phosphorylation of p27. *Cell Death Dis*. 2014;5(7):e1337.
75. Yalcin A, Clem BF, Simmons A, *et al.* Nuclear targeting of 6-phosphofructo-2-kinase (PFKFB3) increases proliferation via cyclin-dependent kinases. *J Biol Chem*. 2009;284(36):24223-24232.
76. Galindo CM, Oliveira Ganzella FA, Klassen G, Souza Ramos EA, Acco A. Nuances of PFKFB3 signaling in breast cancer. *Clin Breast Cancer*. 2022;22(4):e604-e614.
77. Jones BC, Pohlmann PR, Clarke R, Sengupta S. Treatment against glucose-dependent cancers through metabolic PFKFB3 targeting of glycolytic flux. *Cancer Metastasis Rev*. 2022;41(2):447-458.
78. Novellasdemunt L, Obach M, Millan-Arino L, *et al.* Progestins activate 6-phosphofructo-2-kinase/fructose-2,6-bisphosphatase 3 (PFKFB3) in breast cancer cells. *Biochem J*. 2012;442(2):345-356.
79. Ward AV, Matthews SB, Fettig LM, *et al.* Estrogens and progestins cooperatively shift breast cancer cell metabolism. *Cancers (Basel)*. 2022;14(7):1776.
80. Ge T, Yang J, Zhou S, Wang Y, Li Y, Tong X. The role of the pentose phosphate pathway in diabetes and cancer. *Front Endocrinol*. 2020;11(365):365.
81. Li R, Wang W, Yang Y, Gu C. Exploring the role of glucose-6-phosphate dehydrogenase in cancer (review). *Oncol Rep*. 2020;44(6):2325-2336.
82. Patra KC, Hay N. The pentose phosphate pathway and cancer. *Trends Biochem Sci*. 2014;39(8):347-354.
83. Benito A, Polat IH, Noé V, Ciudad CJ, Marin S, Cascante M. Glucose-6-phosphate dehydrogenase and transketolase modulate breast cancer cell metabolic reprogramming and correlate with poor patient outcome. *Oncotarget*. 2017;8(63):106693-106706.

84. Wang J, Duan Z, Nugent Z, *et al*. Reprogramming metabolism by histone methyltransferase NSD2 drives endocrine resistance via coordinated activation of pentose phosphate pathway enzymes. *Cancer Lett*. 2016;378(2):69-79.
85. Monet JD, Thomas M, Dautigny N, Brami M, Bader CA. Effects of 17 beta-estradiol and R5020 on glucose-6-phosphate dehydrogenase activity in MCF-7 human breast cancer cells: a cytochemical assay. *Cancer Res*. 1987;47(19):5116-5119.
86. Thomas M, Bader C, Monet JD. Sex steroid hormone modulation of NADPH pathways in MCF-7 cells. *Cancer Res*. 1990;50(4):1195-1200.
87. Dehdashti F, Mortimer JE, Trinkaus K, *et al*. PET-based estradiol challenge as a predictive biomarker of response to endocrine therapy in women with estrogen-receptor-positive breast cancer. *Breast Cancer Res Treat*. 2009;113(3):509-517.
88. Ellis MJ, Gao F, Dehdashti F, *et al*. Lower-dose vs high-dose oral estradiol therapy of hormone receptor-positive, aromatase inhibitor-resistant advanced breast cancer: a phase 2 randomized study. *JAMA*. 2009;302(7):774-780.
89. Mortimer JE, Dehdashti F, Siegel BA, Trinkaus K, Katzenellenbogen JA, Welch MJ. Metabolic flare: indicator of hormone responsiveness in advanced breast cancer. *J Clin Oncol*. 2001;19(11):2797-2803.
90. Dehdashti F, Flanagan FL, Mortimer JE, Katzenellenbogen JA, Welch MJ, Siegel BA. Positron emission tomographic assessment of "metabolic flare" to predict response of metastatic breast cancer to antiestrogen therapy. *Eur J Nucl Med*. 1999;26(1):51-56.
91. Woitek R, Gallagher FA. The use of hyperpolarised (13)C-MRI in clinical body imaging to probe cancer metabolism. *Br J Cancer*. 2021;124(7):1187-1198.
92. Hagley RD, Moore MR. A progestin effect on lactate dehydrogenase in the human breast cancer cell line T-47D. *Biochem Biophys Res Commun*. 1985;128(2):520-524.
93. Hagley RD, Hissom JR, Moore MR. Progestin stimulation of lactate dehydrogenase in the human breast cancer cell line T-47D. *Biochim Biophys Acta*. 1987;930(2):167-172.
94. Hissom JR, Bowden RT, Moore MR. Effects of progestins, estrogens, and antihormones on growth and lactate dehydrogenase in the human breast cancer cell line T47D. *Endocrinology*. 1989;125(1):418-423.
95. Thomas M, Monet JD, Brami M, *et al*. Comparative effects of 17 beta-estradiol, progestin R5020, tamoxifen and RU38486 on lactate dehydrogenase activity in MCF-7 human breast cancer cells. *J Steroid Biochem*. 1989;32(2):271-277.
96. Macdonald EB, Begovatz P, Barton GP, *et al*. Hyperpolarized (13) C magnetic resonance spectroscopic imaging of pyruvate metabolism in murine breast cancer models of different metastatic potential. *Metabolites*. 2021;11(5):274.
97. Ros S, Wright AJ, D' et *al*. Metabolic imaging detects resistance to PI3Kα inhibition mediated by persistent FOXM1 expression in ER(+) breast cancer. *Cancer Cell*. 2020;38(4):516-533.e19.
98. Xu HN, Kadlececk S, Profka H, Glickson JD, Rizi R, Li LZ. Is higher lactate an indicator of tumor metastatic risk? A pilot MRS study using hyperpolarized (13)C-pyruvate. *Acad Radiol*. 2014;21(2):223-231.
99. Hundshammer C, Braeuer M, Müller CA, *et al*. Simultaneous characterization of tumor cellularity and the Warburg effect with PET, MRI and hyperpolarized (13)C-MRSI. *Theranostics*. 2018;8(17):4765-4780.
100. Gallagher FA, Woitek R, McLean MA, *et al*. Imaging breast cancer using hyperpolarized carbon-13 MRI. *Proc Natl Acad Sci U S A*. 2020;117(4):2092-2098.
101. Woitek R, McLean MA, Gill AB, *et al*. Hyperpolarized (13)C MRI of tumor metabolism demonstrates early metabolic response to neoadjuvant chemotherapy in breast cancer. *Radiol Imaging Cancer*. 2020;2(4):e200017.
102. Fowler AM, Kumar M, Bancroft LH, *et al*. Measuring glucose uptake in primary invasive breast cancer using simultaneous time-of-flight breast PET/MRI: a method comparison study with prone PET/CT. *Radiol Imaging Cancer*. 2021;3(1):e200091.
103. Fowler AM, Strigel RM. Clinical advances in PET-MRI for breast cancer. *Lancet Oncol*. 2022;23(1):e32-e43.